J. Electrochem. Sci. Eng. **14(2)** (2024) 135-145; http://dx.doi.org/10.5599/jese.2061

Open Access : : ISSN 1847-9286
www.jESE-online.org

Original scientific paper

Voltametric and molecular docking investigations of ferrocenylmethylaniline and its N-acetylated derivative interacting with DNA

Asma Yahiaoui[1,2], Benyza-Nabil[2], Amel Messai[3], Touhami Lanez[1,✉] and Elhafnaoui Lanez[1]

[1]*University of El Oued, Chemistry Department, VTRS Laboratory, B.P.789, 39000, El Oued, Algeria*
[2]*University of Khenchela, laboratory of sensors, instrumentations and process, B.P. 1252, 40000 Khenchela, Algeria*
[3]*University of Khenchela, ISMA Laboratory, Faculty of Sciences and Technology, B.P. 1252, 40000 Khenchela, Algeria*

Corresponding author: ✉*touhami-lanez@univ-eloued.dz; Tel.: +213-661-655-550*

Received: September 4, 2023; Accepted: December 1, 2023; Published: December 14, 2023

Abstract

N-ferrocenylmethylaniline (FA) and its N-acetylated derivative (NFA) have been synthesized and fully characterized by various physicochemical techniques such as ^{1}H and ^{13}C NMR spectroscopy. Interactions of FA and NFA with chicken blood DNA were studied by cyclic voltammetry (CV) and molecular docking (MD). The obtained results suggest that both FA and NFA bind strongly via electrostatic interactions to the minor groove of double helix DNA. These electrostatic interactions were evidenced by the findings like a negative formal potential shift in CV and ionic strength effect. The results further show that the binding constants and free binding energies obtained by MD analysis are roughly matched to those obtained from CV. Furthermore, the binding site size was evaluated from voltammetric data.

Keywords

Ferrocene derivatives; DNA minor groove binding; binding site size; binding free energy; docking simulations

Introduction

The foremost cause of all types of cancer is mostly due to abnormal cell proliferation which can alter as a result of changes in nucleotide sequences of DNA, and this can cause the expression of defective proteins that affect regular cellular physiology [1]. DNA also serves as a protein-coding material and its interactions with drugs can change how those proteins are replicated and lead to potential cures for such diseases [2]. Small compounds with potential anticancer activity, such as organometallic compounds, often target DNA within cells and can interact with DNA to cause DNA

damage in cancer cells either directly or through inhibition of enzymes that control DNA integrity or provide building blocks for DNA, preventing cancer cells from proliferating and leading to cell death [3]. Non-specific DNA-targeting organometallic compounds such as cisplatin are among today's most widely, effective, and successful anticancer medications [4].

Research on the anticancer potential of ferrocene derivatives was started in the late 1970s when Brynes and co-workers discovered that ferrocene derivatives bearing amine or amide functions have antitumor action against lymphocytic leukemia [5]. Since then, many other types of ferrocene derivatives have been synthesized and their anticancer activities have been evaluated [6,7]. Ferrocene derivatives such as ferrocenylanilines, in which the aniline group is either directly linked to the ferrocene moiety or separated by a methylene group, are also well known for their valuable pharmacological properties and they have attracted significant interest as potential anticancer and antioxidant drug candidates [8]. Recently, ferrocenylmethylanilines have been considered a potent anticancer agent [9]. Many reports showed that ferrocenylmethylanilines have positive effects on different types of cancer cell lines, such as breast cancer [10].

DNA is a well-known pharmacological target of most drugs currently in clinical use or in advanced clinical trials, when small molecules bind to DNA, they alter or inhibit its function. These small molecules act as drugs when this alteration or inhibition of DNA function is required to cure or control a disease [11].

Since DNA is now known as the primary intracellular target for cancer treatment, the anticancer potential of small molecules has been studied through their interaction with DNA [12].

Therefore, considering the importance of drug-DNA interaction in designing new drug candidates with useful and effective anticancer properties as well as various biological and therapeutic activities, in this work, a study is presented on the interaction of the amine N-ferrocenylmethyl-aniline and its N-acetylated derivative with chicken blood DNA (CB-DNA). Investigations were performed using voltammetry and molecular docking.

Experimental

Material and method

N-ferrocenylmethylaniline (FA) and its N-acetylated derivative (NFA) investigated in this work are shown in Figure 1 and were synthesized by reacting N,N,N-trimethylammoniomethylferrocene iodide[13] with aniline followed by acetylation of the obtained amine, as described below.

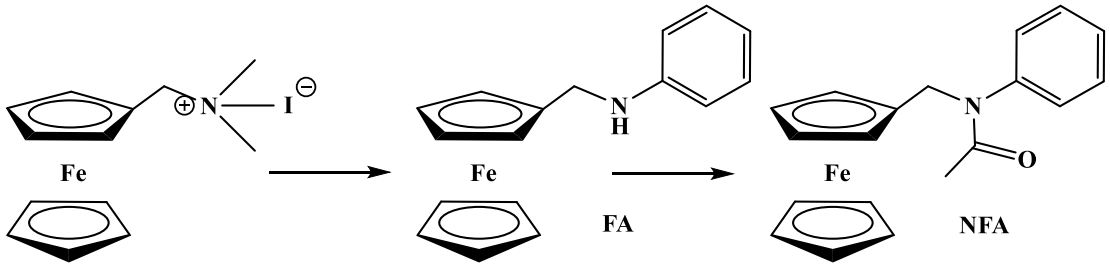

Figure 1. *Reaction scheme and molecular structure of N-ferrocenylmethylaniline (FA) and N-ferrocenylmethyl-N-acetylaniline (NFA)*

Synthesis of N-ferrocenylmethylaniline

The above amine has been synthesized from N,N,N-trimethylammoniomethylferrocene iodide [13] and aniline in water as a solvent. A solution of N,N,N-trimethylammoniomethylferrocene iodide (1 g, 2.6 mmol) in water (20 cm^3) was added dropwise to a solution of aniline (1.4 g,

15.03 mmol) in water (30 cm^3). The mixture was refluxed under nitrogen for 2 hours. Then allowed to cool to room temperature and extracted three times with toluene, the combined toluene layer was dried over magnesium sulphate and evaporated. The obtained residue was recrystallized from a mixture of aqueous ethanol to offer the amine as a yellow leaflet (0.53 g, 69.7 %), melting point (mp) = 85-86 °C.

NMR ^1H (300 MHz, $CDCl_3$): δ = 4.01 ppm (s, 2H, H2), 4.20 ppm (s, 2H, H3), 4.24 ppm (s, 5H, H4), 4.33 ppm (d, 2H, H1), 6.72 ppm (d, 2H, H5), 6.78 ppm (t, 1H, H6), 7.25 ppm (t, 2H, H7), 7.31 ppm (s, 1H, N-H).

NMR ^{13}C (75 MHz, $CDCl_3$) : δ = 44.15 (1C, C1), 68.67 (2C, C2), 68.89 (2C, C3), 69.27 (5C, C4), 87.84 (1C, C5), 113.60 (2C, C7), 118.31 (1C, C9), 130.08 (2C, C8), 149.06 (1C, C6).

Synthesis of N-ferrocenylmethyl-N-acetylaniline

The N-acetyl derivative (0.46 g, 81 %) was obtained by heating the amine N-ferrocenyl-methylaniline (0.5 g, 1.72 mmol) and acetic anhydride (5.1 cm^3) in dry toluene (30 cm^3) at 80 °C for 20 minutes under nitrogen, then poured into water. The toluene layer was separated, dried over magnesium sulphate, and evaporated, and the residue recrystallized from a mixture of aqueous ethanol. The N-acetyl derivative formed yellow plates, mp = 116-117 °C.

NMR ^1H (300 MHz, $CDCl_3$): δ = 1.75 ppm (s, 3H, H8), 4.03 ppm (s, 4H, H2 and H3), 4.08 ppm (s, 5H, H4), 4.61 ppm (s, 2H, H1), 6.99 ppm (d, 2H, H5), 7.28 ppm (t, 1H, H6), 7.32 ppm (t, 2H, H7)

NMR ^{13}C (75 MHz, $CDCl_3$) : δ = 23.55 ppm (1C, C11), 49.12 ppm (1C, C1), 68.86 ppm (2C, C2), 69.27 ppm (5C, C4), 70.62 ppm (2C, C3), 83.86 ppm (1C, C5), 128.60 ppm (2C, C7), 129.28 ppm (1C, C9), 130.16 ppm (2C, C8), 143.56 ppm (1C, C6), 170.47 ppm (1C, C10).

^1H and ^{13}C NMR spectra were obtained on a BRUKER AVANCE DPX 500 MHz spectrometer. Cyclic voltammetry was performed at room temperature (~28 ± 2 °C) using a monocompartment cell with 15 mL capacity. The instrumentation consists of a VoltaLab 40, potentiostat/galvanostat controlled by a microcomputer. The conventional three-electrode system was adopted to perform all the experiments in phosphate buffer solutions. Tetrabutylammonium tetrafluoroborate (Bu_4NBF_4) was used as a supporting electrolyte and its concentration was kept at 0.1 M. The air was removed from the solution by bubbling nitrogen gas through it.

DNA extraction

As described in our previous work [14,15], DNA was isolated from chicken blood, and its stock solution was made by dissolving the DNA in phosphate buffer at pH 7.0, followed by dilution with ethanol to 10 % aqueous ethanol, then it was stored at 4 °C. The concentration of the stock solution was calculated by measuring UV absorbance at λ = 260 nm and using the molar absorption coef-ficient of 6600 M^{-1} cm^{-1} [16].

The evidence that the obtained DNA is protein-free was brought on by measuring the absorbance ratio at λ = 260 and 280 nm, which was 1.97 [17].

The 10 mM stock solutions of FA and NFA were prepared by dissolving the adequate mass of each compound in 5 mL 95 % aqueous ethanol. The solutions were buffered at pH 7 by phosphate buffer (0.1 M KH_2PO_4 + 0.1 M NaOH), this neutral condition prevents the protonation of the ferrocenyl group in strongly acidic conditions [18] and decomposition of the ferrocenium state in basic solutions [19].

Chemicals and reagents

Ferrocene, aniline, acetic anhydride, and tetrabutylammonium tetrafluoroborate were acquired from Sigma-Aldrich and used without purification. All other reagents and solvents were of analytical grade, obtained from different commercial sources and used without further purification. Doubly distilled water was used for all solutions. All the experiments were conducted in 0.1 M phosphate buffer (pH 7) at 28 ± 2 °C. All the results were the average of three experimental measurements.

Cyclic voltammetry measurements

Cyclic voltammetry was measured using a VoltaLab 40 (Radiometer Analytical SAS, France). All assays were carried out in three-electrode electrochemical cells consisting of a saturated calomel electrode as a reference electrode, a platinum wire of thickness 0.5 mm as the counter electrode, and a glassy carbon electrode with an area of 0.077 cm^2 as the working electrode. The voltammogram of a known volume of the solution of each compound was recorded in the absence and presence of a varying concentration of DNA, after flushing out oxygen by bubbling nitrogen gas for 15 minutes. The working electrode was cleaned and polished after every electrochemical assay.

Structural optimization

The structure of the amine and its acetylated derivative used in the molecular docking simulation was fully optimized using density functional theory implemented in the Gaussian 09 package [20] at the theoretical level of B3LYP with two combined basic sets LanL2DZ [21] for optimizing iron atom and 6-311G+(d) for optimizing carbon, hydrogen, oxygen, and nitrogen atoms [22], the fully optimized three-dimensional structures are presented in Figure 2.

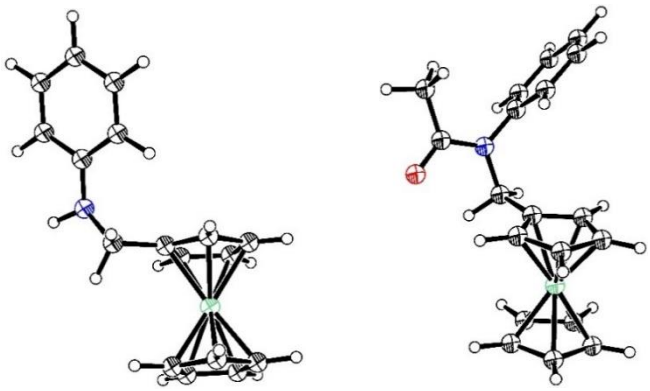

Figure 2. *Fully optimized three-dimensional structures of ligand FA (left) and NFA (right) (ORTEP View 03, V1.08); thermal ellipsoids are plotted at 50 % probability level*

Docking simulations

Molecular docking simulation was performed using AutoDockVina 1.1.2 docking software [23], executed on a personal computer with the following characteristics: Processor: Intel CORE i3-7100U CPU @ 2.40 GHz processor, system memory: 4 GB RAM, system type: 64-bit operating system, Windows 11 as operating system.

Results and discussion

Nuclear magnetic resonance spectral analysis

The ^{1}H NMR spectrums of FA and NFA (Figure 3) reveal two downfield singlets in the range of δ = 4.01-4.20 ppm, which are ascribed respectively to 2- and 3-protons of the substituted cyclopentadienyl ring C_5H_4. The unsubstituted cyclopentadienyl ring C_5H_5 protons appear as a singlet

at 4.24 ppm for FA and 4.08 ppm for NFA. A doublet appeared at δ = 4.33 and 4.61 ppm for FA and NFA, respectively, due to methylene protons. This downfield shift of methylene protons was observed due to the electronegativity of the nitrogen atom. For the proton linked to the nitrogen atom of FA, a singlet was observed at δ = 7.31 ppm, the protons of the methyl group of NFA appeared as a singlet at δ = 1.75 ppm, the aromatic protons appeared in the range of δ = 6.72-7.25 ppm for FA and in the range of 6.99-7.32 ppm for NFA.

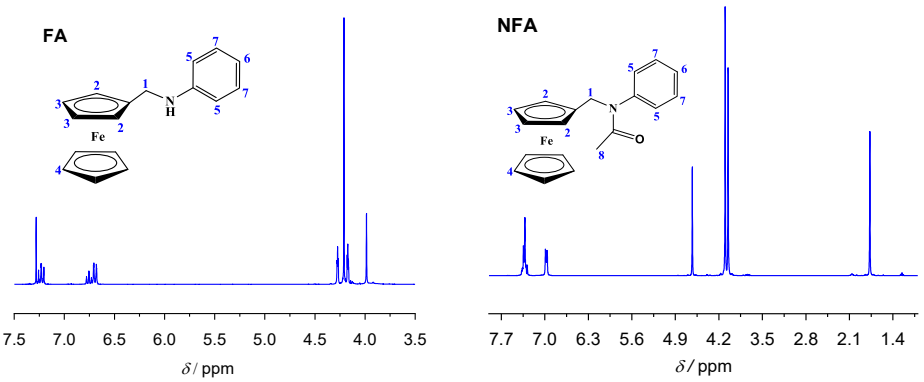

Figure 3. *^{1}H NMR spectra of N-ferrocenylmethylaniline (FA) and N-ferrocenylmethyl-N-acetylaniline (NFA)*

In the ^{13}C NMR spectrum (Figure 4), each carbon atom resonances appears at its characteristic zone according to its carbon atom hybridization. The carbon atom which resonates at δ = 44.15 and 49.12 ppm is associated with the carbon atom of the methylene group. The carbon atoms of the ferrocenyl group resonate between 68.89-87.94 ppm for FA and in the range of 68.86-83.86 for NFA, whereas the carbon atoms of the aromatic rings are observed between 113.60-149.06 ppm for FA and in the range of 128.60 to143.56 ppm for NFA. The carbon of the methylene group is observed at 44.15 and 49.12 ppm for the amine and its acylated form, respectively.

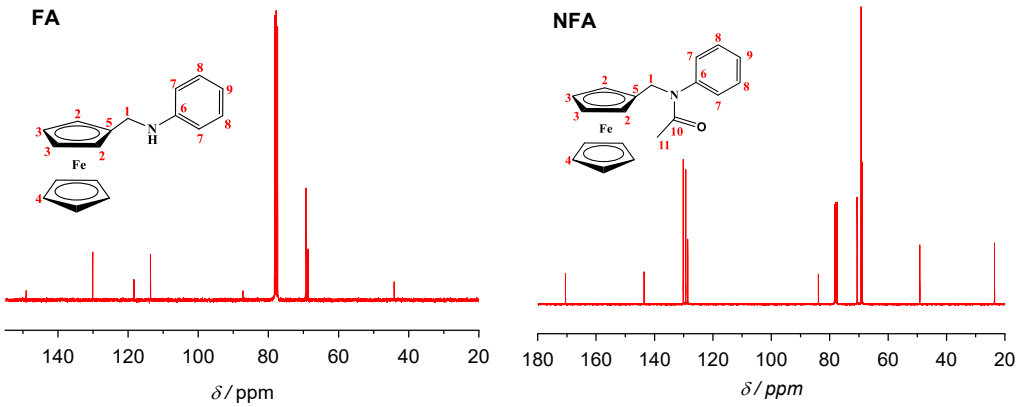

Figure 4. *^{13}C NMR spectra of N-ferrocenylmethylaniline (FA) and N-ferrocenylmethyl-N-acetylaniline (NFA)*

Cyclic voltammetry studies

The cyclic voltammetry behavior of 3 mM FA and NFA in the presence of gradually increasing concentration of CB-DNA at a bare glassy carbon electrode is shown in Figure 5. Upon addition of CB-DNA into FA or NFA solution, the anodic peak potential was shifted in the negative going direction and anodic peak current density was remarkably decreased. The significant decrease in peak current density can be attributed to the formation of the slowly diffusing adducts FA-DNA and NFA-DNA, which lower the concentration of the free ligands FA and NFA responsible for charge transfer reactions. The shift in the anodic peak potential in the negative going direction is attributed to the physical interaction between ligands and CB-DNA [24].

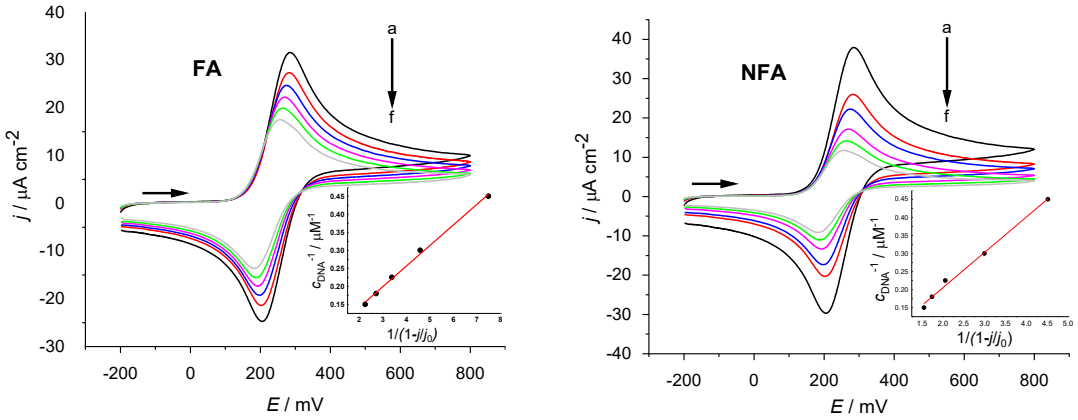

Figure 5. *Cyclic voltammograms of 3 mM phosphate buffer solution of FA and NFA in the absence (a) and presence of 2 (b), 3 (c), 4 (d), 5 (e) and 6 µM (f) of CB-DNA recorded at 0.1 V s^{-1} potential scan rate. Inset: plots of c_{DNA}^{-1} vs. 1/1-(j/j_0)*

The binding constants of the investigated compounds were calculated from the decrease in the anodic peak current density of FA-DNA and NFA-DNA adducts relative to free FA and NFA, respectively, using equation (1) [25]:

$$\frac{1}{c_{DNA}} = \frac{K_b(1\text{-}A)}{1\text{-}(j/j_0)}\text{-}K \quad (1)$$

where A is the proportionality constant, K_b is the binding constant, j and j_0 are the anodic peak current densities in the presence and absence of DNA, and c_{DNA} is DNA concentration. Linear equations were obtained from the plot of c_{DNA}^{-1} *vs.* 1/1-(j/j_0) (inset of Figure 5) with a linear correlation coefficient of 0.995. This suggested that the binding number was 1, thus, the inclusion complexes interacted with CB-DNA to form a 1:1 association complex. The values of the binding free energy of the ligands FA and NFA with CB-DNA were obtained using binding constants obtained from the y-intercept of the linear equation, and their values were found to be -27.15 and -29.76 kJ mol^{-1}, respectively, as shown in Table 1.

Table 1. *The linear equations of c_{DNA}^{-1} vs. 1/1-(j/j_0), binding constant, and binding free energy values of FA-DNA and NFA-DNA obtained from CV data at pH 7.2 and T= 301 K*

Adduct	Equation	R^2	K_b / M^{-1}	-Δ*G* / kJ mol^{-1}
FA-DNA	*y* = 0.06*x* - 0.0028	0.995	5.7×10^4	27.15
NFA-DNA	*y* = 0.163*x* - 0.0465	0.995	16.3×10^4	29.76

Binding site size

The binding site size (*s*) was calculated based on equation (2) [26]:

$$\frac{c_b}{c_f} = K_b\left(\frac{\text{free base pairs}}{s}\right) \quad (2)$$

where *s* represents the binding site size in terms of base pair, K_b is the binding constant, c_f is the concentration of the free compound, and c_b represents the concentration of the DNA-bound compound. As the concentration of a DNA base pair is given in terms of nucleotide phosphate, the concentration of the DNA base pair will be expressed as $c_{DNA}/2$ and hence, equation (2) can be written as equation (3):

$$\frac{c_b}{c_f} = K_b\frac{c_{DNA}}{2s} \quad (3)$$

The c_b/c_f ratio is equal to (j_0-j) / j [27], which are the values of experimental peak current densities. The plots of c_b/c_f versus c_{DNA} are displayed in Figure 6.

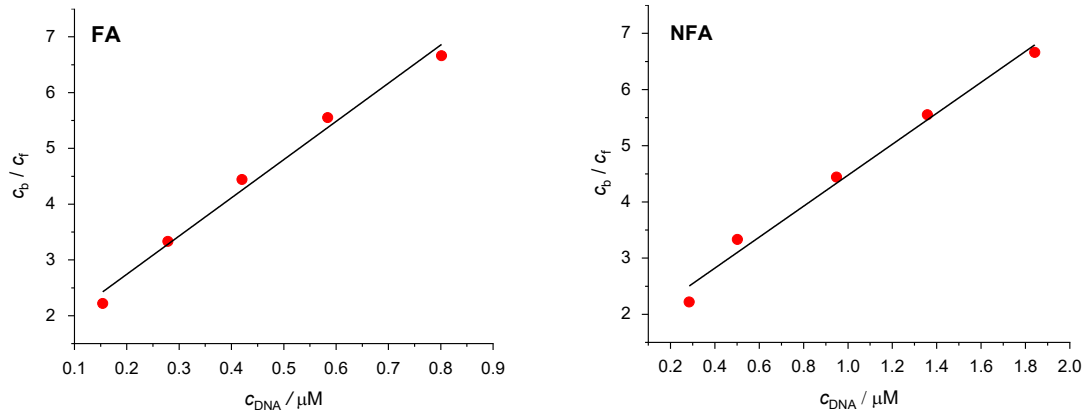

Figure 6. *Plots of c_b/c_f versus c_{DNA} for FA and NFA, used for the calculation of binding site size*

The equations obtained by least squares fitting in the studied concentration range for FA and NFA are shown in Table 2 (where *y* represents the value of the c_b/c_f ratio and *x* the compound concentration, expressed in µM).

Table 2. *Values of binding site size obtained using the plot of c_b/c_f versus C_{DNA}*

Adduct	Equation	R^2	*s* (base pair)
FA-DNA	$y = 6.85x + 1.372$	0.983	0.004
NFA-DNA	$y = 2.75x + 1.719$	0.982	0.029

The small values of binding site size further suggest that FA and NFA interact electrostatically with CB-DNA.

Effect of ionic strength on the interaction of FA and NFA with CB-DNA

Generally, the ionic strength of the reaction medium has a substantial impact on the strength of the electrostatic interaction. In this section, the ionic strength on the binding propriety of FA and NFA was evaluated by adding various concentrations of NaCl solution to a 3 mM solution of DNA with and without 4 µM of FA and NFA. Upon NaCl addition, the anodic current peak densities of the complexes DNA-FA and DNA-NFA gradually decreased as the concentration of NaCl was increased from 0 to 80 mM, indicating the existence of electrostatic interaction as presented in Figure 7.

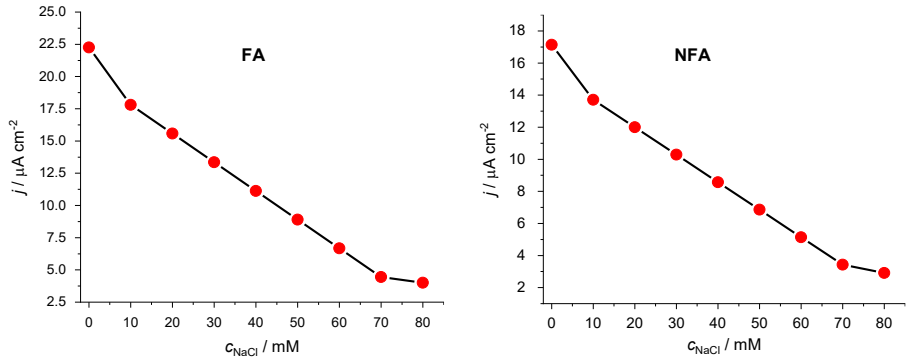

Figure 7. *Influence of the ionic strength of NaCl on the anodic current peak densities of DNA-FA and DNA-NFA complexes*

Molecular docking studies

To simulate the interaction between the target DNA and the test compounds, molecular docking simulation was performed using AutoDockVina 1.1.2 docking software [27]. The 3D-crystal structure

of DNA sequence d(CGCGATATCGCG) dodecamer (ID: 1DNE), shown in Figure 8, was obtained from the online protein data bank (https://www.rcsb.org/pdb) was used as a target [28].

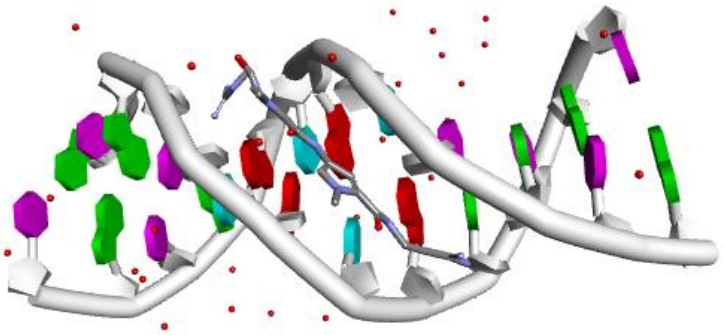

Figure 8. *3D-crystal structure of DNA sequence d(CGCGATATCGCG) 2 dodecamer (ID: 1DNE)*

Furthermore, polar hydrogen atoms and Gasteiger charges were added to the target by AutoDock 4.2 docking software [29]. Then, the Lamarckian genetic algorithm method was used to search for the binding position in the DNA target, and the grid points were determined based on covering the whole of the DNA target. All other parameters were set as default. The lowest energy conformation obtained from the ligand-target complex was considered the predicted binding mode and compared with the experimental results. The output from docking studies was rendered with Discovery Studio [30] to visualize the DNA-ligand interactions. Figure 9 presents the lowest energy docking poses of the compounds FA and NFA inserted into the minor groove at the G/C - rich region of the oligonucleotide.

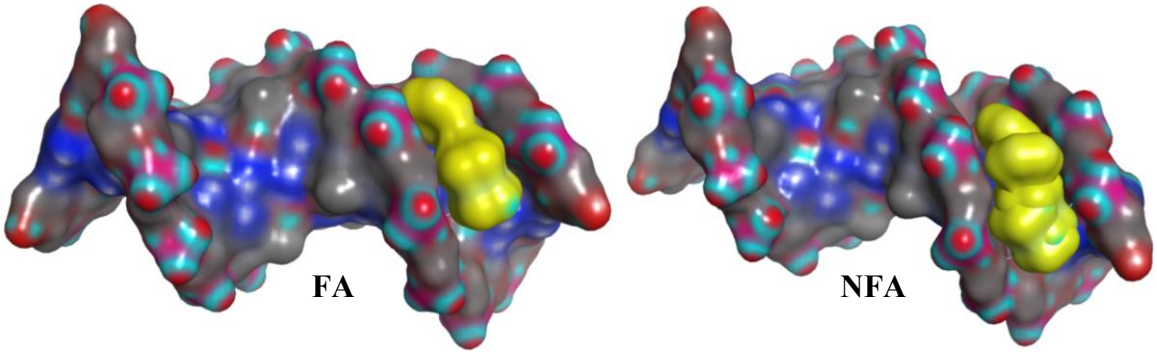

Figure 9. *Surface view of the docked pose of FA and NFA (yellow color) with DNA (PDB ID: 1DNE) illustrating the insertion of FA and NFA in the minor groove of DNA*

The stable conformation corresponding to the lowest binding energy was used for docking analysis. The visualization of the interaction was generated with Discovery Studio [30]. Results from molecular docking suggest that hydrogen bonding interactions are involved in the binding process. NFA had the highest negative binding energy. It interacted with the target DNA (1DNE) *via* three conventional hydrogen bonds with the nucleotides DG16, DG10, and DC11. However, the compound FA interacted only *via* two conventional hydrogen bonds with the nucleotides DC11 and DG10. Table 3 summarizes the interacting nucleotides and their corresponding bond types and length with the binding energy.

Figure 10 illustrates the 3D binding mode of FA and NFA with the nearby nucleotides in the active site of DNA.

The results obtained from molecular docking were entirely in agreement with the experimental data obtained from cyclic voltammetry.

Table 3. *Hydrogen bonding, binding constant, and binding free energy values of FA-DNA and NFA-DNA adducts obtained from molecular docking analysis data*

Adduct	Nucleotide	Distance, nm	K_b / M^{-1}	-Δ*G* / kJ mol^{-1}
FA-DNA	DC11	25.6	6.21×10^4	27.30
	DG10	24.8		
NFA-DNA	DG16	24.7	17.22×10^4	29.82
	DG10	27.0		
	DC11	19.3		

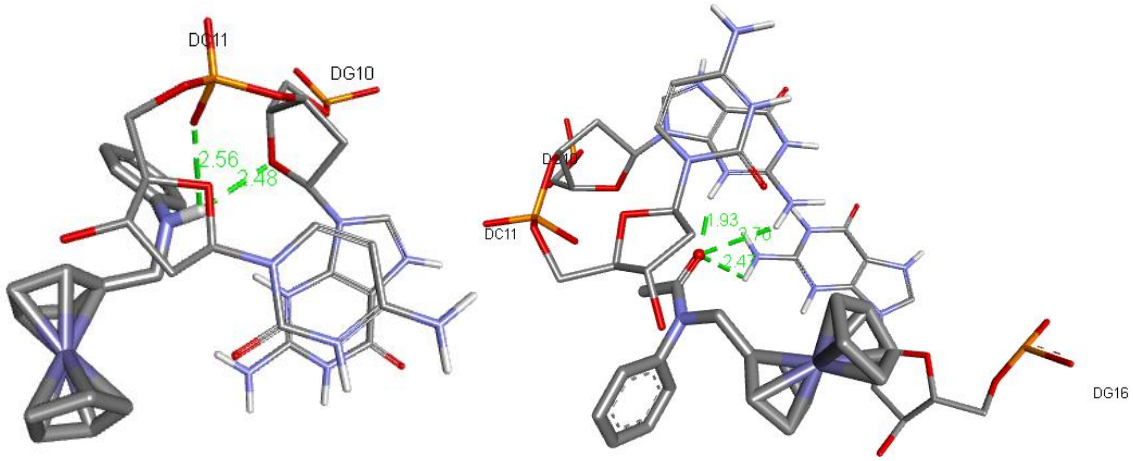

Figure 10. *3D binding mode of the FA and NFA with DNA (PDB ID: 1DNE), hydrogen bonds are denoted by green dashed line*

Conclusions

In this paper, the binding affinity of N-ferrocenylmethylaniline (FA) and its N-acetylated derivative (NFA) with chicken blood DNA (CB-DNA) have been studied. The results suggest that both compounds bind to CB-DNA *via* groove binding mode. The interaction evidence is supported by the following findings:

1) the results showed that the obtained binding free energy by cyclic voltammetry 27.15 and 29.76 kJ mol^{-1} for FA and NFA, respectively, is matched roughly to the binding free energy that was calculated by the molecular docking study 27.3 and 29.82 kJ mol^{-1};
2) decrease of the peak current density of the FA and NFA upon adding the CB-DNA;
3) the results of CV and ionic strength effect indicated the electrostatic interaction of both compound FA and NFA with CB-DNA as the dominant mode. The same mode of interaction was also supported by the results obtained from molecular docking.

Acknowledgements*: This work was supported by the Directorate-General of Scientific Research and technological Development (DGRSDT) and the Laboratory of Valorization and Technology of Saharan Resources (VTRS) (project code: B00L01UN390120150001).*

References

[1] J. F. Alhmoud, J. F. Woolley, A.-E. Al Moustafa, M.I. Malki, DNA Damage/Repair Management in Cancers, *Cancers* (Basel) **12** (2020) 1050. https://doi.org/10.3390/cancers12041050
[2] N. Chowdhury, A. Bagchi, An Overview of DNA-Protein Interactions, *Current Chemical Biology* **9** (2016) 73-83. https://doi.org/10.2174/2212796809666151022202255
[3] M. R. Shorkaei, Z. Asadi, M. Asadi, Synthesis, characterization, molecular docking and DNA binding studies of Al(III), Ga(III) and In(III) water-soluble complexes, *Journal of Molecular Structure* **1109** (2016) 22-30. https://doi.org/https://doi.org/10.1016/j.molstruc.2015.12.070

[4] S. Ghosh, Cisplatin, The first metal based anticancer drug, *Bioorganic Chemistry* **88** (2019) 102925. https://doi.org/10.1016/j.bioorg.2019.102925
[5] V. J. Fiorina, R. J. Dubois, S. Brynes. Ferrocenyl polyamines as agents for the chemoimmunotherapy of cancer, *Journal of Medicinal Chemistry* **21** (1978) 393-395. https://doi.org/10.1021/jm00202a016
[6] N. Zegheb, C. Boubekri, T. Lanez, E. Lanez, In Silico Study on N-Ferrocenylmethyl-N-Phenylpropionohydrazide and N-Ferrocenylmethyl-N-Pheylbenzohydrazide as Anticancer Drugs for Breast and Prostate Cancer, *International Journal of Pharmacology, Phytochemistry and Ethnomedicine* **11** (2018) 17-25. https://doi.org/10.18052/WWW.SCIPRESS.COM/IJPPE.11.17
[7] A. Khennoufa, L. Bechki, T. Lanez, E. Lanez, N. Zegheb, Spectrophotometric, voltametric and molecular docking studies of binding interaction of N-ferrocenylmethylnitroanilines with bovine serum albumin, *Journal of Molecular Structure* **1224** (2021) 129052. https://doi.org/10.1016/j.molstruc.2020.129052
[8] A. Kedadra, T. Lanez, E. Lanez, H. Hemmami, M. Henni, Synthesis and antioxidant activity of six novel N-ferrocenylmethyl-N-(nitrophenyl)- and -N-(cyanophenyl)-acetamides: Cyclic voltammetry and molecular docking studies, *Journal of Electrochemical Science and Engineering* **12** (2022) 293-304. https://doi.org/10.5599/jese.1162
[9] T. Lanez, E. Lanez, A Molecular Docking Study of N-Ferrocenylmethylnitroanilines as Potential Anticancer Drugs, *International Journal of Pharmacology, Phytochemistry and Ethnomedicine* **2** (2016) 5-12. https://doi.org/10.18052/www.scipress.com/IJPPE.2.5
[10] N. Zegheb, C. Boubekri, T. Lanez, E. Lanez, T. T. Küçükkılınç, E. Öz, A. Khennoufa, S. Khamouli, S. Belaidi, In Vitro and In Silico Determination of Some N-ferrocenylmethylaniline Derivatives as Anti-Proliferative Agents Against MCF-7 Human Breast Cancer Cell Lines, *Anti-Cancer Agents in Medicinal Chemistry* **22** (2022) 1426-1437. https://doi.org/10.2174/1871520621666210624141712
[11] O. Kennard, DNA-drug interactions, *Pure and Applied Chemistry* **65** (1993) 1213-1222. https://doi.org/10.1351/pac199365061213
[12] N. Shahabadi, A. Fatahi, Multispectroscopic DNA-binding studies of a tris-chelate nickel(II) complex containing 4,7-diphenyl 1,10-phenanthroline ligands, *Journal of Molecular Structure* **970** (2010) 90-95. https://doi.org/10.1016/j.molstruc.2010.02.048
[13] J. M. Osgerby, P. L. Pauson, 128. Ferrocene derivatives. Part VI. DL-ferrocenylalanine, *Journal of the Chemical Society (Resumed)* (1958) 656-660. https://doi.org/10.1039/JR9580000656
[14] T. Lanez, H. Benaicha, E. Lanez, M. Saidi, Electrochemical, spectroscopic and molecular docking studies of 4-methyl-5-((phenylimino)methyl)-3H- and 5-(4-fluorophenyl)-3H-1,2-dithiole-3-thione interacting with DNA, *Journal of Sulfur Chemistry* **39** (2018) 76-88. https://doi.org/10.1080/17415993.2017.1391811
[15] E. Lanez, L. Bechki, T. Lanez, Computational molecular docking, voltammetric and spectroscopic DNA interaction studies of 9N-(Ferrocenylmethyl)adenine, *Chemistry and Chemical Technology* **13** (2019) 11-17. https://doi.org/10.23939/chcht13.01.011
[16] R. Vijayalakshmi, M. Kanthimathi, V. Subramanian, B.U. Nair, DNA cleavage by a chromium(III) complex, *Biochemical and Biophysical Research Communications* **271** (2000) 731-734. https://doi.org/10.1006/bbrc.2000.2707
[17] J. A. Glasel, Validity of nucleic acid purities monitored by 260nm/280nm absorbance ratios, *Biotechniques* **18** (1995) 62-63.
[18] Anthony J. Pearson, *Metallo-organic chemistry*, Chichester [West Sussex] ; New York, John Wiley & Sons, 1985. ISBN: 978-0471904403

[19] C.-S. Lu, X.-M. Ren, C.-J. Hu, H.-Z. Zhu, Q.-J. Meng, The Inclusion Compound of a New Ionizable Derivative of b b-Cyclodextrin with Ferrocenium Drug, *Chemical and Pharmaceutical Bulletin* **49** (2001) 818-821. https://doi.org/10.1248/cpb.49.818
[20] M. Frisch, G. Trucks, H. Schlegel, G. S. Wallingford, U. CT, U. 2009, Gaussian 09; Gaussian, Inc, Gaussian, (2016). https://gaussian.com/g09citation
[21] C. Chizallet, S. Lazare, D. Bazer-Bachi, F. Bonnier, V. Lecocq, E. Soyer, A.-A. Quoineaud, N. Bats, Catalysis of Transesterification by a Nonfunctionalized Metal−Organic Framework: Acido-Basicity at the External Surface of ZIF-8 Probed by FTIR and ab Initio Calculations, *Journal of the American Chemical Society* **132** (2010) 12365-12377. https://doi.org/10.1021/ja103365s
[22] M. Shahsavari, S. Tajik, I. Sheikhshoaie, H. Beitollahi, Fabrication of Nanostructure Electrochemical Sensor Based on the Carbon Paste Electrode (CPE) Modified with Ionic Liquid and Fe_3O_4/ZIF-67 for Electrocatalytic Sulfamethoxazole Detection, *Topics in Catalysis* **65** (2022) 577-586. https://doi.org/10.1007/s11244-021-01471-8
[23] O. Trott, A. J. Olson, AutoDock Vina: Improving the speed and accuracy of docking with a new scoring function, efficient optimization, and multithreading, *Journal of Computational Chemistry* **30** (2009) 455-461. https://doi.org/10.1002/jcc.21334
[24] N. Li, Y. Ma, C. Yang, L. Guo, X. Yang, Interaction of anticancer drug mitoxantrone with DNA analyzed by electrochemical and spectroscopic methods, *Biophysical Chemistry* **116** (2005) 199-205. https://doi.org/10.1016/j.bpc.2005.04.009
[25] G.-C. Zhao, J.-J. Zhu, J.-J. Zhang, H.-Y. Chen, Voltametric studies of the interaction of methylene blue with DNA by means of β-cyclodextrin, *Analytica Chimica Acta* **394** (1999) 337-344. https://doi.org/10.1016/S0003-2670(99)00292-5
[26] M. Aslanoğlu, N. Öge, Voltametric, UV Absorption and Viscometric Studies of the Interaction of Norepinephrine with DNA, *Turkish Journal of Chemistry* **29** (2005) 477-485. https://journals.tubitak.gov.tr/chem/vol29/iss5/3
[27] M. Aslanoglu, G. Ayne, Voltammetric studies of the interaction of quinacrine with DNA, *Analytical and Bioanalytical Chemistry* **380** (2004) 658-663. https://doi.org/10.1007/s00216-004-2797-5
[28] M. Coll, J. Aymami, G. A. van der Marel, J. H. van Boom, A. Rich, A. H. J. Wang, Molecular structure of the netropsin-d(CGCGATATCGCG) complex: DNA conformation in an alternating AT segment, *Biochemistry* **28** (1989) 310-320. https://doi.org/10.1021/bi00427a042
[29] G. M. Morris, H. Ruth, W. Lindstrom, M. F. Sanner, R. K. Belew, D. S. Goodsell, A. J. Olson, Software news and updates AutoDock4 and AutoDockTools4: Automated docking with selective receptor flexibility, *Journal of Computational Chemistry* **30** (2009) 2785-2791. https://doi.org/10.1002/jcc.21256
[30] BIOVIA, Dassault Systems, Discovery Studio Visualizer, v21.1.1.020289, San Diego: Dassault Systems, 2020. https://www.3ds.com/products/biovia/all-products